TECHNICAL ANALYSIS REPORT No: 9/02

OCCURRENCE No: 200105627

REFERENCE No: BE/200100029

Analysis of a failed Pratt & Whitney JT9D-7R4 turbofan engine

Boeing 767-238, VH-EAQ

27 November 2001

ANALYSIS OF A FAILED PRATT & WHITNEY JT9D-7R4 TURBOFAN ENGINE

BOEING 767-238, VH-EAQ, 27 NOVEMBER 2001

EXECUTIVE SUMMARY

The left engine of a Boeing 767-238 aircraft (VH-EAQ) failed during the climb phase of a regular passenger transport flight from Melbourne to Sydney. After the failure, which was characterised by a single loud 'bang' and severe vibration, the engine was shut down and the aircraft returned to Melbourne.

Engineering inspections of the JT9D-7R4 engine found that one of the fan blades had failed part-way along its length and impacted the fan case at the 11 o'clock position, causing the failure of several nose-cowl bolts and substantial damage to components adjacent to the impact point. After the initial impact, the failed blade struck the inside of the nose cowl, forward of the fan. This impact was of sufficient energy to puncture the nose cowl and allow the escape of the blade segment. No damage was caused externally to the airframe or control surfaces.

ATSB laboratory examination of the blade section remaining within the fan rotor disk found that the blade had fractured as a result of fatigue crack growth from a pre-existing defect at the blade trailing edge. The defect was identified as a shallow crack that had formed during or before the last blade refurbishment operation, carried out in 1991. Non-destructive examination procedures carried out on the blade following the refurbishment had failed to detect the defect.

In 1998, the manufacturer purchased the engine for use as a lease unit. The defective blade was installed into the engine shortly thereafter. At the time of failure, the blade had operated for 7,187 hours and through 2,083 cycles following its 1991 refurbishment. Operating times and cycles before the blade refurbishment were not available.

Neville R. Blyth

Senior Transport Safety Investigator
Technical Analysis

ANALYSIS OF A FAILED PRATT & WHITNEY JT9D-7R4 TURBOFAN ENGINE

BOEING 767-238, VH-EAQ, 27 NOVEMBER 2001

1. FACTUAL INFORMATION

1.1 Introduction

On the morning of November 27 2001, Boeing 767-238 aircraft VH-EAQ sustained the failure of the left (number-one) engine during a regular passenger transport flight from Melbourne to Sydney. The flight and cabin crews described the failure as being characterised by a single loud 'bang' accompanied by severe airframe vibration. At the time of the failure, the aircraft was climbing through an altitude of 16,000 feet. After shutting down and securing the failed engine, the flight crew returned the aircraft to Melbourne airport and carried out an uneventful single-engine approach and landing.

Initial inspections by airport ground personnel found severe damage to the engine nose-cowl and fan assembly, including several holes where debris had passed through the cowl (figure 1). The engine fan had lost the majority of one complete blade, with many others showing severe impact damage and distortion along the tip edges (figures 2 & 3). A blade opposite to the fractured item had lost material from the tip.

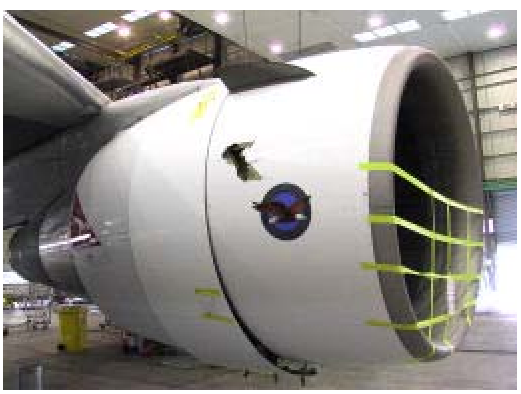

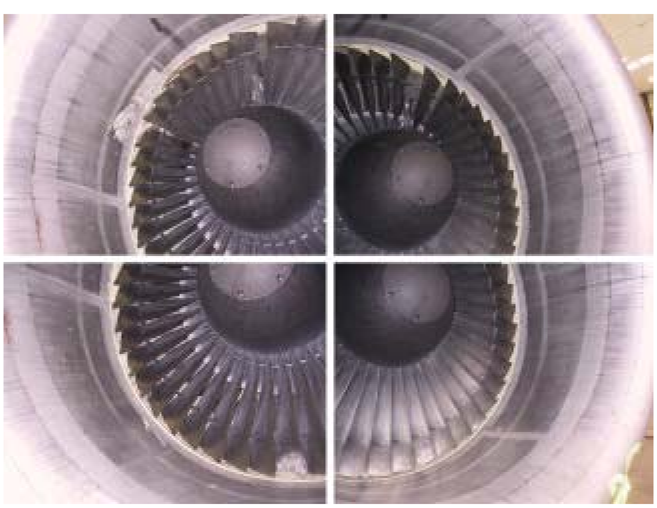

Fig. 1 (Top L). Right side of the failed engine, showing the nose-cowl puncture.

Fig. 2 (Top R). Intake of the engine – general view.

Fig. 3 (Left). Montage image of the engine fan and intake internal surfaces.

1.2 Engine history

The Pratt & Whitney JT9D-7R4 engine (serial number P716610) was first purchased as a lease unit by Pratt & Whitney in 1998 and had since been installed on several aircraft from various different airlines. The engine was installed into the number-one (left) position on VH-EAQ during a heavy maintenance check in October 2001. At the time of failure, the engine had operated for a total of 26,138 hours and through 8,900 cycles. The last 319 hours and 200 cycles had been accumulated while the engine was installed on VH-EAQ.

1.3 Blade history

The failed fan blade (part number 5001341-022, serial number ND9278) was first installed into engine P716610 in August 1998, after being in storage since 1991. Before being placed in storage, the blade had undergone a number of repairs (see section 1.7.1), including two elevated temperature straightening operations where the blade was heated to 650ºC and the airfoil shape re-formed. The manufacturer's records indicated the blade subsequently operated for 7,187 hours and through 2,083 cycles while installed in engine P716610. The total time and cycles on the blade since manufacture were unknown.

1.4 Blade inspection history

Information from the engine manufacturer indicated that non-destructive inspection procedures (eddy-current) were carried out after the blade straightening operation in 1991. Following its reintroduction into service within engine P716610, periodic blade examinations were required to comply with the engine maintenance manual, however records of these inspections for the time the engine was with previous operators were not available.

Immediately prior to the installation of the engine on VH-EAQ, the fan assembly underwent an inspection for foreign object damage, an eddy-current inspection of the blade leading edges and a re-lubrication of the part-span shroud contact faces. No further formal inspections were required or carried out during the ensuing 319 hours of operation before the engine failure.

1.5 External engine damage

The operator, in conjunction with the ATSB, carried out a general inspection of the failed engine before it was removed from the aircraft. The majority of the physical damage was associated with the failed fan blade, which had fractured transversely at a location around 250 millimetres above the rotor connection. Most of the fracture surface showed angled surfaces typical of ductile shear, however a flat, uniform region extending 85 millimetres forward from the trailing edge presented chevron markings and evidence of progressive crack growth (see section 1.7.2). The remainder of the blades showed signs of appreciable rocking and lateral movement within their sockets, with many of the part-span shroud platforms having sustained appreciable damage over the contacting faces (figure 4). Several of the blades had locked together at the shrouds and the forward shroud from the blade behind the failed item had broken away under bending loads (figure 5). The blade diametrically opposite the fractured item had lost around 25 millimetres of material from the tip edge, with the associated fractures showing features typical of ductile shear and tearing (figure 6).

Fig. 4 (Top L). Damage to the contact surfaces of the fan part-span shrouds.

Fig. 5 (Top R). Breakage of the rear part-span shroud from the blade adjacent to the failed item.

Fig. 6 (Left). Blade opposite to the failed item , showing the degree of metal loss from the tip.

The inspection found no evidence of impact damage to the blade at or below the point of failure. Most other blades presented deformation of the tip edges and leading edge chipping, typical of debris impact. Several of the outlet guide vanes behind the fan also carried impact damage (figure 7) and a large section of the intake lining from behind the fan had lifted and folded up against the vane edges (figure 8). The attrition lining around the blade path showed severe wear and gouging for the full circumference and contained an angled impact mark immediately below the mounting point of the fan speed (N1) sensor (figure 9). The orientation of the impact mark matched the pitch angle of the blade aerofoil tip. Inspection on the outside of the fan case revealed a large outward bulge associated with the impact location, as well as damage to an adjacent wiring loom. The N1 sensor itself was not present – all mounting bolts had failed in overload and the cowling above the sensor position had a 50 x 100 millimetre hole punctured through to the outside (figure 10). Along the right side of the fan case, the strengthening rib had buckled slightly and showed deformation associated with the distortion of the fan case (figure 11). A vibration sensor from the low-pressure compressor assembly was recovered loose from within the right fan cowling, having broken away from the engine casing and wiring looms.

The composite spinner assembly showed a small (10mm x 10mm) chip adjacent to the spinner cap (figure 12). The appearance and localised nature of the chip was consistent with foreign object impact damage.

Fig. 7 Impact damage to the engine outlet guide vanes.

Fig. 8 Lifting of a section of the bypass duct lining in front of the outlet guide vanes.

Fig. 9 (Top) Principal impact point of the failed blade on the fan case.

Fig. 11 (Bottom) Buckling and distortion of a fan case rib, below the impact point.

Fig. 10 (Top) N1 sensor location and the hole through the fan cowl panel immediately above.

Fig. 12 (Bottom) Suspected foreign object impact point on the engine spinner.

1.6 Structural damage

Structural damage associated with the engine failure was limited to the engine nacelle. Despite evidence that a number of fragments or components had been forcefully liberated from the engine, the inspections found no damage to the fuselage, wings or control surfaces of the aircraft.

Externally, the nose-cowl of the JT9D engine contained a single large penetration near the three o'clock position (figures 13 & 14). Measuring approximately 300mm x 150mm and around 200mm forward of the edge of the fan case, the perforation represented the exit point of a large piece of debris (presumably the outer section of the fan blade) as it was liberated from the rotating assembly. The internal impact point was around the two-o'clock position and showed progressive crushing of the internal honeycomb structure as the debris (blade) impacted and then passed through the cowl wall with a tangential trajectory (figure 15). A repair panel adjacent to the upper section of the internal puncture also showed damage typical of a glancing impact with debris. Two other internal penetrations of the nose-cowl were evident at the five and six o'clock positions, however neither of these damaged areas extended through to the external surface.

Figs. 13 & 14 External perforation of the engine nose-cowl and damage to the composite outer skin.

Fig. 15 Internal damage to the engine nose cowl, leading to the perforation shown in figures 13 & 14. Upper panel is a previous repair.

Fig. 16 Location of several nose cowl bolts fractured during the blade separation event.

Four nose-cowl lip bolts on the right side of the engine had fractured under radial shear loads (figure 16), with significant associated elongation of the fan case mounting holes and the adjoining cowl structure (figure 17). Several of the bolt heads and washers were recovered loose inside the fan-cowls, including two items that had forcefully embedded into the cowl inside surface (figure 18). Other damage to the fan-cowls included the 50 x 100 millimetre puncture above the N1 speed sensor position and a smaller 20 x 20 millimetre perforation at the 2 o'clock position, caused by another of the failed nose-cowl lip bolts (figure 19).

Fig. 17 Elongation of the nose cowl mounting flange bolt holes.

Fig. 18 Nose cowl bolt head and washer embedded into the underside of the right fan cowl.

Fig. 19 Small puncture in the right fan cowl caused by a fractured nose cowl bolt head.

1.7 Blade failure

Upon completion of the general inspections, the fractured and adjacent blades were removed from the engine and individually examined, along with their respective root sockets in the fan rotor disk. All of the dovetail root connections examined showed no evidence of abnormal socket interaction, with no significant galling or fretting noted (figures 20 & 21). Quantities of dry lubricant compound were present over the root and socket surfaces – some of this had migrated outward under centrifugal forces, dispersing over the blade aerofoil surfaces.

Measurement of the failed blade's chord width at the point of failure (181.14mm) found it to be below the minimum specified dimension (182.12mm) for the particular distance above the root (z-plane) at which the fracture had occurred (288mm) [1]. This was attributed to an area of localised material removal from a previous trailing edge blending operation (figure 22).

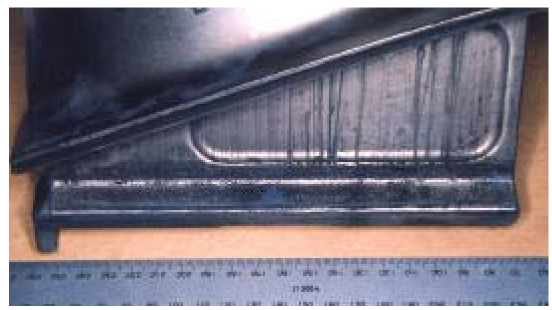

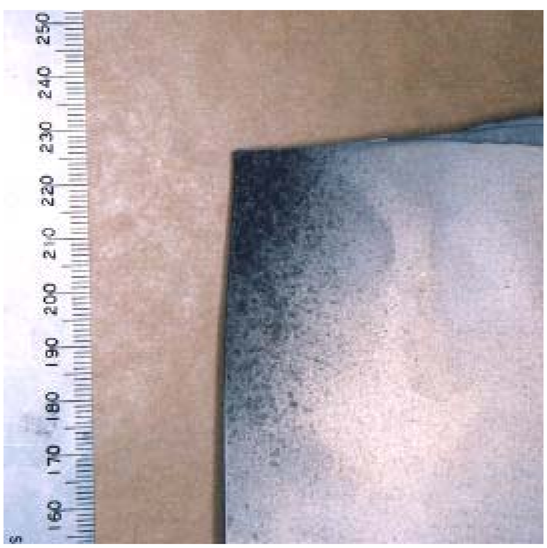

Figs. 20 & 21 (Top) Blade dove-tail root surfaces – free from significant galling and fretting damage and showing remnant dry lubricant.

Fig. 22 (Left) Trailing edge of the failed blade around the point of fracture initiation. Note the thinning of the section width attributed to a prior blending operation.

[1]P&W JT9D Engine Manual, #72-31-02 INSP/CHK-01 Min Blade Chord Length

1.7.1 Identification markings

The failed blade carried the following engraved identification on the root underside (fig 23).

SY4 WCT ~~B352~~ 5001341-022 ~~798511~~ 36
21 B284 SB72-117 ND9278

Fig. 23 Blade identification on the root face.

On the upper surface of the blade platform, repair codes as follows were engraved (figures 24 & 25). The meaning of the various codes as identified by the manufacturers engine manual are shown opposite[2].

(A) STCT-2	?	Second straightening procedure by Chem-Tronics company
DA	?	Part-span shroud wear
STCT	?	First straightening procedure by Chem-Tronics company
DC-1	?	Leading-edge tip patch repair
DC-2	?	Trailing-edge tip patch repair
DC-3	?	Leading edge adjacent to shroud, patch repair

Figs. 24 & 25 Blade repair codes present on the upper surface of the flange.

[2] P&W JT9D Engine Manual, #72-31-02 REPAIR-13 Mark Repair Codes

1.7.2 Fracture surface

As evident during the general inspection, the failed blade had fractured through the aerofoil section, approximately 280mm / 190mm above the blade root platform at the leading and trailing edges. The fracture presented two characteristic zones – a flat region of progressive fatigue cracking extending for 85 millimetres from the trailing edge, and an angular ductile shear fracture (typical of tensile overload) for the remainder of the section (figure 26 & 27).

Fig. 26 Full blade fracture surface, with trailing edge to the right.

Fig. 27 Tapering region of fatigue cracking, with a prominent arrest mark (arrowed).

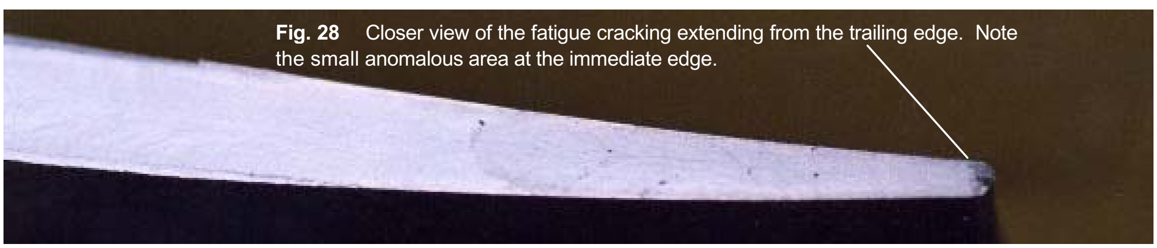

Fig. 28 Closer view of the fatigue cracking extending from the trailing edge. Note the small anomalous area at the immediate edge.

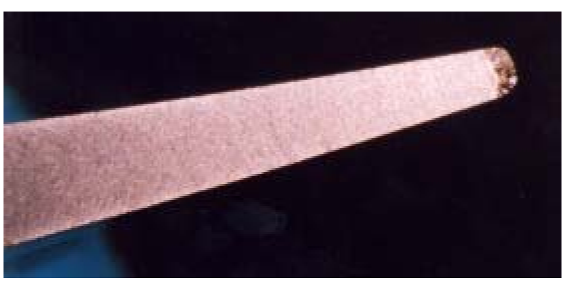

Fig. 29 (Above) Low-magnification view of the early stages of the fatigue cracking – vague arrest marks evident radiating out from the blade edge.

Fig. 30 (Right) Defect at the blade edge , showing tinting consistent with elevated temperature exposure.

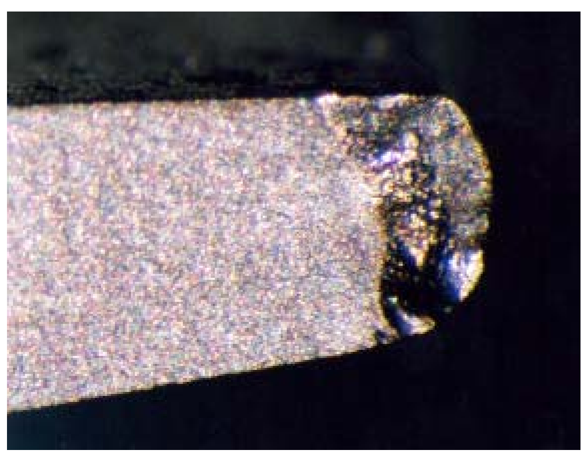

Low-power stereomicroscopic examination of the fatigued region found approximately eight to fifteen arrest lines between the trailing edge and the ductile shear transition. The definition and spacing of the marks generally increased with distance from the trailing edge, with the majority being present within the first fifteen millimetres of cracking. The most prominent arrest mark was found at a distance of 28 millimetres from the trailing edge (figure 28). All arrest marks and general fracture morphology indicated fatigue crack initiation from the immediate trailing edge of the blade. At elevated magnifications, an isolated region was identified at that point and extended to a depth of 0.62 millimetres (figures 29 & 30). The region showed a clear transition to the area of fatigue cracking and also showed evidence of elevated temperature oxidation (heat tinting).

Scanning electron microscopy of the trailing edge fatigue origin identified two sub-regions with distinctly different morphologies (figures 31 & 32). The outermost zone (depth of 260µm) presented an irregular, dimpled surface - characteristic of ductile tensile overload failure (figure 33). Beneath this area was a 350µm deep zone of rubbed, smeared surface (figure 34). Neither of the regions showed any evidence of material defects or the influence of external (foreign object) damage. Both regions also showed light surface oxidation, consistent with the heat tinting observed visually. Electron imaging of the trailing edge leading up to the fracture showed no signs of impact damage or other discontinuities that could have been associated with the initiation of fatigue cracking (figure 35).

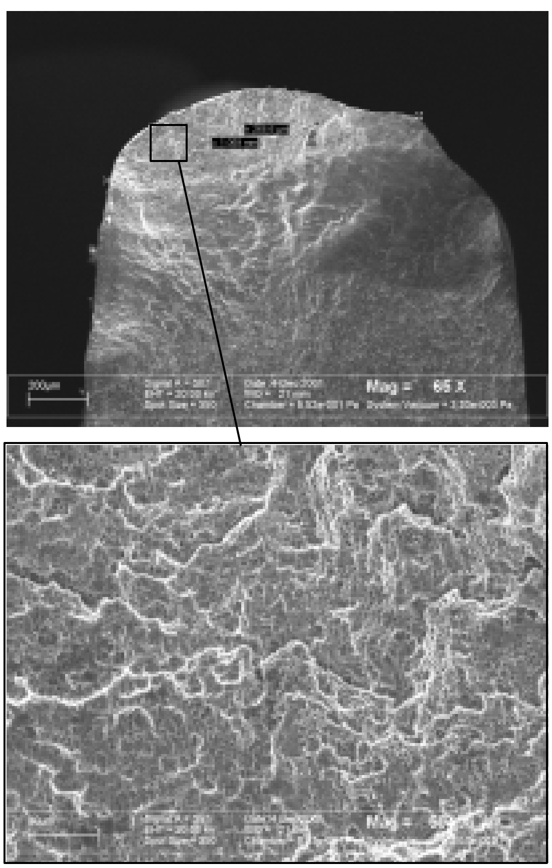

Figs 31 & 33 (Above) Dimensions and morphology of the outer region of the edge defect. Features typical of ductile tensile fracture.

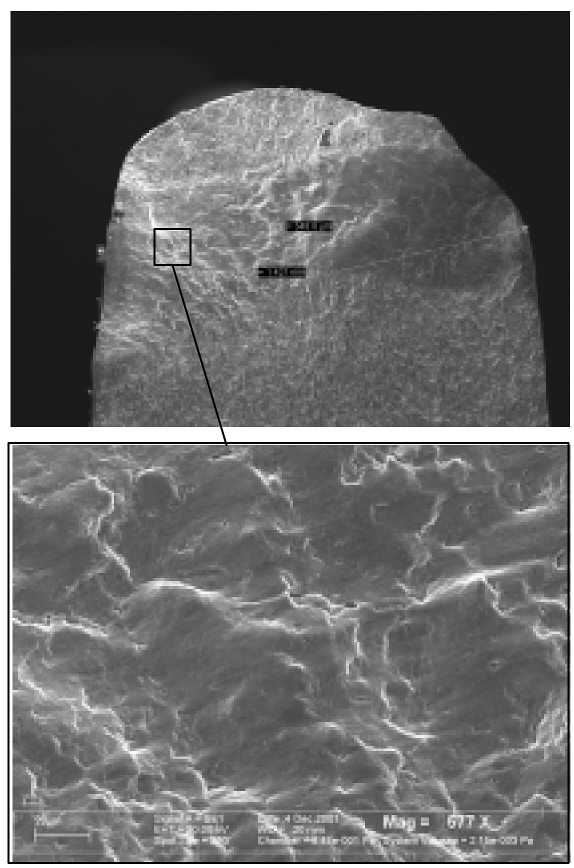

Figs 32 & 34 (Above) Dimensions and morphology of the inner region of the edge defect. Typically rubbed and flowed surfaces.

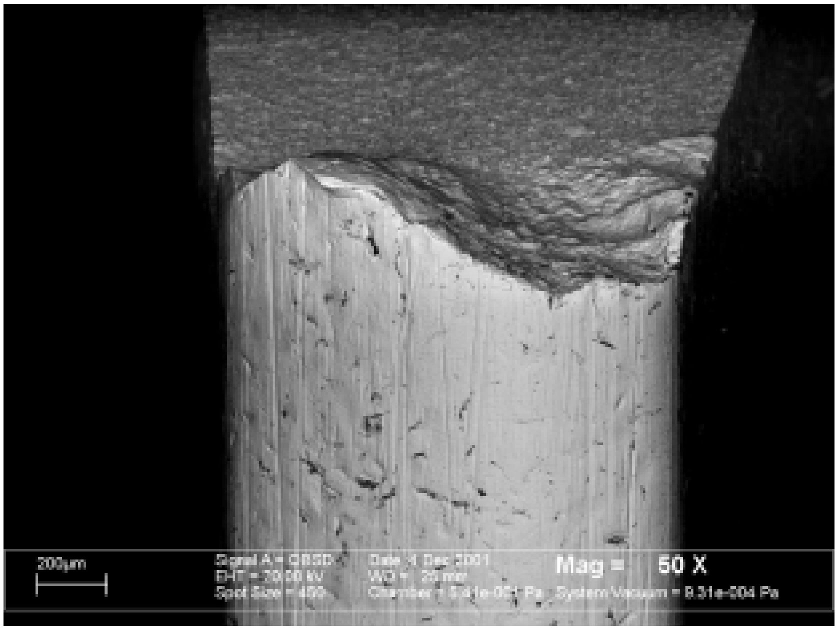

Fig. 35 Electron image of the blade trailing edge at the fatigue origin. The area was completely absent of any indications of mechanical or impact (foreign object) damage.

1.7.3 Microstructure

The area of trailing edge blade material encompassing the fatigue origin was removed and prepared as a planar metallographic section. Progressive grinding to approximately one-half of the section thickness was followed by conventional polishing and optical examination in the etched and unetched conditions.

At no location along or beneath the fracture profile at the fatigue origin did the blade material exhibit any microstructural anomaly or other metallurgical feature that could have contributed to the initiation of fatigue cracking (figure 36). Cracking was predominantly transgranular and showed little evidence of branching. The material microstructure was typical of a forged and heat-treated Ti6Al4V material, showing preferentially oriented α grains in a fine α-β matrix. The structure was uniform throughout the sample examined.

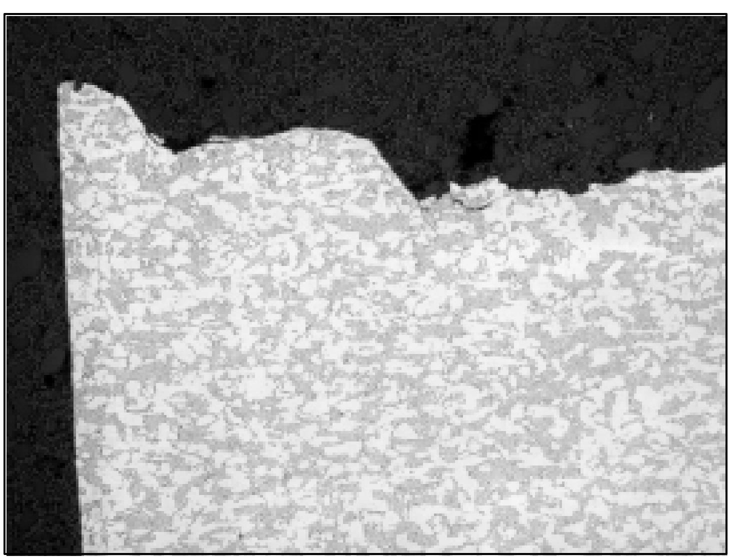

Fig. 36 Metallographic cross-section taken through the fatigue origin. The microstructure was typical of the blade material and the origin area completely free of any inclusions, anomalous structures or other material-related defects. Kroll's reagent etch. Magnification X140

2. ANALYSIS

Failure of the left engine from VH-EAQ had occurred as a direct result of the fatigue fracture and liberation of a single low-pressure compressor (fan) blade. The initiation of fatigue cracking commenced from a pre-existing, 0.6mm deep defect in the blade trailing edge, located 288 millimetres axially above the root face. The defect location was at the centre of a previous blend repair to the blade trailing edge. Dimensional inspection found that this repair had resulted in the chord-wise width of the blade being reduced to around one millimetre below the specified minimum. While this depth of blending was considered undesirable, it was not considered of sufficient magnitude to have contributed significantly to the subsequent development of the fatigue cracking from the trailing edge defect. Numerous fracture surface arrest marks extending outward from the initiation site suggested that the cracking had developed over multiple flight cycles, with initiation and growth under vibratory and centrifugal operating forces. Final ductile overload failure of the blade had occurred after the growth of the fatigue cracking to a total length of 85 millimetres, measured along the blade centreline.

The physical characteristics of the initiation site identified it as a crack-like feature formed under localised tensile loads. 'Heat-tinting' (oxidation) of the defect surfaces indicated their exposure to elevated temperatures associated with the aerofoil straightening procedures that were carried out twice during the life of the blade. As such it was evident that the defect existed before, or was formed during the straightening procedures. Routine non-destructive procedures carried out following the blade re-work had failed to detect the presence of the trailing edge defect before the blade was re-introduced into service within engine P716610.

All damage to the engine cowls and low-pressure compressor instrumentation was consistent with the transient shock loads associated with the impact of the fractured blade against the fan case. The fan case itself had successfully contained the blade, however the liberated segment had subsequently moved forward and struck the nose cowl with sufficient remaining energy to puncture and pass through the cowl structure.